NeuroImage 197 (2019) 273–283

Contents lists available at ScienceDirect

NeuroImage

journal homepage: www.elsevier.com/locate/neuroimage

Subjective vividness of motor imagery has a neural signature in human premotor and parietal cortex

Adam Zabicki [a,*], Benjamin de Haas [c], Karen Zentgraf [d,b], Rudolf Stark [b], Jörn Munzert [a], Britta Krüger [a,b]

[a] Neuromotor Behavior Laboratory, Institute of Sport Sciences, Justus Liebig University Giessen, Germany
[b] Bender Institute of Neuroimaging, Justus Liebig University Giessen, Germany
[c] Experimental Psychology, Justus Liebig University Giessen, Germany
[d] Institute of Sport and Exercise Sciences, Goethe University Frankfurt, Germany

ARTICLE INFO

Keywords:
Vividness of imagery
Motor imagery
MVPA
RSA

ABSTRACT

Motor imagery (MI) is the process in which subjects imagine executing a body movement with a strong kinesthetic component from a first-person perspective. The individual capacity to elicit such mental images is not universal but varies within and between subjects. Neuroimaging studies have shown that these inter-as well as intra-individual differences in imagery quality mediate the amplitude of neural activity during MI on a group level. However, these analyses were not sensitive to forms of representation that may not map onto a simple modulation of overall amplitude. Therefore, the present study asked how far the subjective impression of motor imagery vividness is reflected by a spatial neural code, and how patterns of neural activation in different motor regions relate to specific imagery impressions. During fMRI scanning, 20 volunteers imagined three different types of right-hand actions. After each imagery trial, subjects were asked to evaluate the perceived vividness of their imagery. A correlation analysis compared the rating differences and neural dissimilarity values of the rating groups separately for each region of interest. Results showed a significant positive correlation in the left vPMC and right IPL, indicating that these regions particularly reflect perceived imagery vividness in that similar rated trials evoke more similar neural patterns. A decoding analysis revealed that the vividness of the motor image related systematically to the action specificity of neural activation patterns in left vPMC and right SPL. Imagined actions accompanied by higher vividness ratings were significantly more distinguishable within these areas. Altogether, results showed that spatial patterns of neural activity within the human motor cortices reflect the individual vividness of imagined actions. Hence, the findings reveal a link between the subjective impression of motor imagery vividness and objective physiological markers.

1. Introduction

Imagery is a multifaceted and completely subjective phenomenon. Mental images can have very different qualities (i.e., visual, tactile, proprioceptive, motor) and are a central element of human experience. Imagery in the context of motor actions (i.e., motor imagery, MI) refers to a process in which subjects imagine the execution of a body movement with a strong kinesthetic component from a first-person perspective. Thus, the subject imagines "being inside his or her body" and "experiencing those sensations" (Roberts et al., 2008). Therefore, a motor image is a conscious motor representation containing functional and causal properties of the imagined movement (Munzert and Zentgraf, 2009).

A broad body of literature suggests that the neural substrate of motor images is organized around several core and broader motor regions: the supplementary motor area (SMA), different sections of the premotor cortex (dPMC, vPMC), the primary motor cortex (M1), posterior parietal regions such as the inferior (IPL) and the superior parietal lobe (SPL), the basal ganglia (BG), and the cerebellum (Guillot et al., 2008; Lotze et al., 1999; for a review, Munzert et al., 2009). Because both the dorsal premotor area and the superior section of the posterior parietal lobe are associated with motor planning and internal modeling, they seem to play a particularly major role in creating motor images (for a review, Fogassi and Luppino, 2005; for a review, Rizzolatti and Matelli, 2003; Wolpert et al., 1998). These results stem to a large extent from traditional

* Corresponding author. Institute for Sport Science, Justus Liebig University Giessen, Kugelberg 62, 35394, Giessen, Germany.
E-mail address: adam.zabicki@sport.uni-giessen.de (A. Zabicki).

https://doi.org/10.1016/j.neuroimage.2019.04.073
Received 9 November 2018; Received in revised form 17 April 2019; Accepted 27 April 2019
Available online 30 April 2019

univariate studies investigating the local magnitude of activity in specialized neurons or brain regions. Alternative, newer approaches use multivariate pattern analysis (MVPA) such as pattern classification techniques (Haxby et al., 2001; Haynes, 2011; Kamitani and Tong, 2005) or representational similarity analysis (RSA) (Kriegeskorte and Kievit, 2013; Kriegeskorte et al., 2008) to infer the representational properties of neural populations in a region of the cortex from the similarity of activation patterns in an abstract feature space. Studies using MVPA have demonstrated that distributed neural response patterns in motor and motor-related areas can be used to distinguish whether they have been elicited by the execution, imagery (Park et al., 2015), or observation of a hand action (Filimon et al., 2015). Further studies have distinguished between different imagined hand actions based on their underlying neural activation patterns (Pilgramm et al., 2016; Zabicki et al., 2016). However, little is known about how the brain represents the individual impression of the imagery experience.

In an applied context, mentally rehearsing movements has become an important technique for athletes and patients (for a review, Lotze and Halsband, 2006; Murphy, 1994). For example, mental practice with MI improves motor task performance and learning (Braun et al., 2013; Feltz and Landers, 1983). Behavioral research (e.g., Isaac, 1992) has demonstrated a moderating effect of vividness of imagery on motor performance, with participants who report more vivid imagery showing greater performance improvements. Thus, individual differences in imagery ability relate to the effectiveness of imagery (e.g., Isaac and Marks, 1994; Mantani et al., 2005). Several questionnaires (e.g., the Vividness of Movement Imagery Questionnaire [VMIQ], VMIQ-2) characterize imagery ability as the achieved vividness; that is, the clarity and realism of the imagery experience (Baddeley and Andrade, 2000; Roberts et al., 2008). The ability to create such vivid motor images can be considered as both a trait and a state variable. This notion is underpinned by previous neuroscientific studies showing that both inter- and intra-individual differences in imagery ability and quality mediate the amplitude of neural activity during MI on a group level (Guillot et al., 2008; Lebon et al., 2012; Lorey et al., 2011; Mizuguchi et al., 2016). These studies demonstrated, for example, that: (a) good imagers show a stronger activation in the parietal and ventrolateral premotor regions (Guillot et al., 2008): (b) activity in V1 depends on the capability of kinesthetic motor imagery (Mizuguchi et al., 2016); (c) higher imagery vividness is parametrically associated with an increased BOLD response within the putamen, the premotor cortex (PMC), the posterior parietal cortex, the primary motor cortex, the somatosensory cortex, and the left cerebellum (Lorey et al., 2011); and (d) the facilitation of corticomotor excitability during MI correlates positively with individual imagery ability (Lebon et al., 2012). These results help us to understand that imagery vividness is related to the overall magnitude of BOLD responses or the differential excitability of brain regions. However, multivariate approaches are sensitive to forms of representation that may not map onto a simple modulation of overall amplitude. As a result, they may reveal vividness representations that would go undetected in univariate studies. They can further help us to understand the space in which information is represented in a region; that is, how the patterns of neural activation in different motor regions relate to specific imagery impressions and how the representations of different impressions relate to each other. Characterizing the representational geometry of regional activity patterns may not only detect *where* such representations are to be found in the brain but also shed light on *how* MI vividness is represented neurally. Representational mapping, therefore, emphasizes the relationships between experiential properties such as those of MI impressions with different levels of vividness along with their distances in high-dimensional space as defined by the collective patterns of voxel activity (Kriegeskorte et al., 2008; Kriegeskorte and Kievit, 2013).

In the present study, we used a multivariate approach to test whether the representation of a motor image within frontal and parietal motor regions (dPMC, vPMC, SPL, IPL, IPS, M1) relates to the perceived vividness of the respective motor image. Specifically, we examined whether patterns of activity in the human motor cortices correspond to differences along the vividly perceived–nonvividly perceived motor image dimension and where this relation is represented in the human motor cortices. We asked subjects to imagine different right-hand actions: aiming, extension–flexion, and squeezing (Lorey et al., 2013; Pilgramm et al., 2016; Zabicki et al., 2016). After each trial, we asked them to rate the perceived vividness of the respective motor image. We then applied a representational similarity analysis (RSA) (Kriegeskorte et al., 2008). This used representational dissimilarity matrices (RDMs) to characterize the representational geometry of motor images with different perceived vividness in every motor region (Kriegeskorte et al., 2008; Kriegeskorte and Kievit, 2013). To gain information on the correlation between the similarity–dissimilarity relation of the self-reported vividness experience and the representational geometry of activity patterns during motor imagery, we compared these RDMs with the structure of ratings of perceived vividness. Via this analysis, we investigated whether similarly rated trials were accompanied by similar neural patterns, and whether this association between ratings and neural patterns differs between our regions of interest (ROIs). In addition, we performed a decoding analysis (cf. Zabicki et al., 2016) to test whether neural patterns for specific imagined hand movements depend on subjective vividness ratings. Here, we tested the hypothesis that more vividly imagined hand movements would elicit an action-specific neuronal pattern, whereas less vividly imagined movements would be noisier and therefore elicit a less action-specific neural pattern, resulting in lower levels of decoding accuracy.

2. Materials and methods

2.1. Subjects

Twenty right-handed volunteers (14 female, mean age = 22.9 years, $SD = 2.9$) with normal or corrected-to-normal vision participated in this experiment. All participants showed generally good imagery ability in the VMIQ-2 (Roberts et al., 2008) (first-person kinesthetic imagery: mean VMIQ-2 score = 2.18, $SEM = 0.17$; third-person visual imagery: mean VMIQ-2 score = 2.28, $SEM = 0.15$, $r = 0.673$, $p < 0.01$). They reported no history of psychiatric or neurological disorders as well as no history or current use of any psychoactive medication. The study was approved by the local ethics committee of the Psychology and Sport Science Department of the Justus Liebig University Giessen in Germany, and all subjects gave informed written consent in accordance with the Declaration of Helsinki. The study took place at the Bender Institute of Neuroimaging (BION, Justus Liebig University, Germany).

2.2. Design and task

The experiment contained seven conditions: three imagery, three execution, and one rest. In the present paper, we address only the imagery phases. For further information on the execution conditions, see Zabicki et al. (2016).

Before the fMRI experimental phase, subjects completed a familiarization session (see below). In the imagery conditions, they were instructed to imagine one of three tasks: (a) a force production task squeezing a bellows, (b) an aiming task pointing with the index finger at five targets affixed to the bellows, or (c) an extension–flexion movement with the right hand (i.e., the fingers) alongside the bellows (Fig. 1A). The aiming task required no memorizing of a spatial sequence of targets, because subjects were instructed to simply imagine pointing to five affixed targets one after another (Lorey et al., 2014; Pilgramm et al., 2016; Zabicki et al., 2016). During the imagery and rest conditions, subjects kept their eyes closed.

During the fMRI experimental phase, subjects were scanned in a 3-T whole-body scanner (see below). Conditions were presented in a pseudorandomized order counterbalanced across subjects. Each trial started with a written instruction presented for 2.5 s (*"Imagine Squeezing Hand,"*

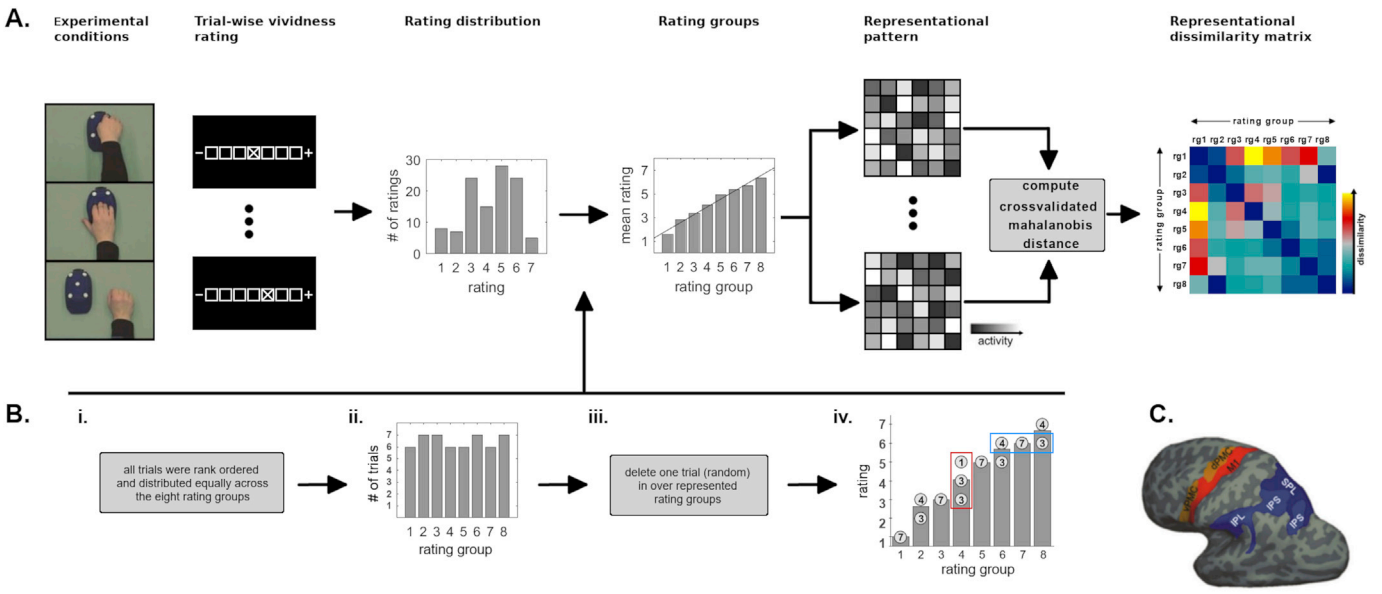

Fig. 1. Representational dissimilarity analysis. From experimental conditions to representational dissimilarity matrices. (A) Each motor imagery trial is rated according to its perceived vividness on a scale ranging from 1 (*low vividness*) to 7 (*high vividness*). The resulting rating distribution is transformed into eight rating groups, each containing an equal number of experimental trials. The response patterns in a brain region for different rating groups are compared to determine the associated representational dissimilarity. The dissimilarity between two patterns is measured as the cross-validated Mahalanobis distance, and assembled in the brain RDM. (B) To create the rating groups from the rating distribution (i), all trials are rank ordered and distributed as equally as possible into eight groups (ii). In over-represented groups, one randomly selected trial is discarded (iii), before calculating the mean rating value of the trials in each rating group (iv). Note that another randomization step was necessary, because a total of 14 six-rated trials (blue frame) have to be randomly distributed over three different rating groups. Depending on the subject's rating behavior, a specific rating group may contain trials with different vividness ratings (red frame). (C) The brain picture shows the anatomical location of ROI labels on the reconstructed surface of an example hemisphere. M1: primary motor cortex, dPMC: dorsal premotor cortex, vPMC: ventral premotor cortex, SPL: superior parietal lobule, IPS: intraparietal sulcus, IPL: inferior parietal lobule, CSF: cerebrospinal fluid.

"Imagine Aiming Hand," "Imagine Rhythmic Movement Hand," or "Close Your Eyes and Rest") followed by a jitter (0–90% of TR) and the respective imagery or rest phase (8 s). Instructions were presented with a PC running Presentation software (Neurobehavioral Systems, Albany, USA) and projected onto a screen behind the scanner that could be viewed through a mirror attached to the head coil. During imagery and rest, subjects kept their eyes closed, reopening them only when the MI or rest phase was finished. This was signaled by a sound. After each trial, subjects were asked to rate and confirm (max. 3 s) the perceived quality (i.e., the perceived vividness) of their imagery or execution performance on a 7-point scale ranging from *very high* (7) to *very low* (1). They were also asked to give ratings after the rest trial in order to keep the stimulation of the subjects similar in each trial and experimental condition. Here, participants were instructed to rate how well they had relaxed.

Each subject performed 10 runs of eight trials each (corresponding to two trials in each of the four conditions) in each of two separate scanning sessions within one week. This amounted to a total of 20 runs, 160 trials, and a scanning time of approximately 45 min. To control for involuntary movements during MI trials, we recorded the surface EMG sum potential from two target muscles of the right forearm during scanning (*M. flexor carpi radialis* and *M. palmaris longus*).

2.3. Familiarization session

Prior to the first fMRI scanning session, subjects filled out the *Vividness of Movement Imagery Questionnaire-2* (Roberts et al., 2008) and the *Edinburgh Handedness Inventory* (Oldfield, 1971) before completing a preparatory session to familiarize themselves with the different experimental conditions and the experimental setting. First, they observed and executed the different movements (see above) before imagining them. All subjects were trained to imagine the different hand movements from a first-person perspective. More precisely, participants were instructed to imagine the movements as if they were performing them, thereby including kinesthetic as well as visual aspects of the movement. We used MATLAB (MathWorks Inc., Massachusetts, USA) to simulate the forthcoming fMRI session and monitored EMG signals from several target muscles of the right forearm using a real-time biofeedback system (Biofeedback 2000 x-pert, Schuhfried GmbH, Mödling, Austria). This procedure allowed us to give subjects feedback on whether they performed MI without any notable muscle contraction. After each training trial, subjects rated the quality (i.e., the perceived vividness) of their imagery on a 7-point scale ranging from *very high* (7) to *very low* (1). This session lasted a total of 30 min.

2.4. Image acquisition and preprocessing

The fMRI data were collected on a 3-T whole-body scanner (Siemens Prisma, Erlangen, Germany) with a standard 20-channel head coil. We acquired one structural image from each participant consisting of 176 T1-weighted sagittal images (1-mm slice thickness; MPRAGE) at the first session as well as a fieldmap (40 slices; TE(1): 10 ms; TE(2): 12.46 ms; TR: 1000 ms) for the separate scanning sessions. For the run of functional imaging, a total of 1260 vol were registered using a T2*-weighted gradient echo-planar imaging sequence (EPI) with 40 slices covering the whole brain (slice thickness = 3 mm; 0.75 mm gap; descending; time of acquisition (TA) = 2.4375 s; time of repetition (TR) = 2.5 s; time of echo (TE) = 30 ms; flip angle = 87°; field of view = 192 mm × 192 mm). The orientation of the axial slices was parallel to the AC–PC line. Trial onsets were jittered within 0–90% of the TR.

Image preprocessing was carried out using SPM 12 (Wellcome Department of Imaging Neuroscience, University College London, UK). Origin coordinates were adjusted to the anterior commissure. Furthermore, realignment and unwarping were performed using voxel displacement maps generated from the fieldmaps (Hutton et al., 2002), and the functional images were co-registered with the anatomical scan for the respective subject. Smoothing was executed using an isotropic

three-dimensional Gaussian filter with a full-width-at-half-maximum (FWHM) kernel of 5 mm.

2.5. Data analysis

2.5.1. Individual rating behavior

First, we investigated individual rating behavior in order to (a) determine its stability across the two scanning sessions, and (b) test for possible individual differences. Therefore, in a first step, we calculated the correlations between the mean, the variance, and the range of the ratings used by each participant across sessions, as well as the average *root mean squared deviation* (RMSD) between the eight rating groups (see below) of the two sessions for each subject. Second, we calculated the occurrence of each rating value per participant for each session separately. All pairwise differences between rating value occurrences were calculated and stored in a 7×7 matrix, leading to 20 rating behavior matrices per session (one per subject). In the next step, we compared each subject's Session 1 matrix with the same subject's Session 2 matrix by calculating Pearson's r of the lower triangle entries, leading to a second-order subject similarity matrix (SSM, see Charest et al., 2014). Next, we calculated within-subject (average of SSMs diagonal entries) and between-subject (average of SSMs lower triangle entries) rating behavior replicability values. We assessed statistical significance with a randomization of the rating value labels corresponding to a null hypothesis that all rating values would be equally represented. This null hypothesis was simulated by a random permutation of the rating values, reordering rows and columns of one of the two rating behavior matrices to be compared according to this permutation, and computing the randomized average within-subject and between-subject correlations of the randomized matrices. We repeated this procedure 10,000 times, leading to a randomization distribution of within- and between-subject correlations, simulating the null hypothesis that the matrices were unrelated. The null hypothesis would be rejected if the actual behavior matrices (i.e., the ones with consistent labeling between the two matrices) fell within the top 5% of the simulated null distributions of correlations. A p value of $p < 0.0001$ would indicate that the actual correlation was higher than any of the 10,000 correlations obtained after randomization of the rating value labels.

To test for individual differences (i index) in rating behavior (i.e., whether the within-subject replicability of the matrices was larger than the between-subject replicability), we computed the difference between the average within- and the average between-subject replicability. Under the null hypothesis that all subjects would show the same rating behavior, subject labels were exchangeable (and did not need to match when calculating within- and between-subject correlations). Thus, statistical significance was assessed by randomization (again 10,000 repetitions) of the subject labels (for the second session only, to destroy the match between subjects).

2.5.2. Regions of interest

The anatomical scan was used to reconstruct the cortical surface of each hemisphere using FreeSurfer (version 5.3, http://surfer.nmr.mgh.harvard.edu). Regions of interest (ROIs) were selected on the basis of previous findings reported in the MI literature (Ehrsson et al., 2003; Grezes and Decety, 2001; Heed et al., 2011; Jeannerod, 2001) and defined anatomically on an individual basis using the FreeSurfer parcellation algorithm (Destrieux et al., 2010; cf. Pilgramm et al., 2016). We defined six ROIs (Fig. 1C) per hemisphere as follows:

1. Primary *motor* cortex (**M1**), defined as the precentral gyrus
2. Dorsal and ventral *premotor* cortex (**dPMC** and **vPMC**), defined as the superior and inferior part of the precentral sulcus respectively
3. Superior (**SPL**) and inferior *parietal* lobule (**IPL**), defined as the supramarginal and the angular gyrus as well as the intraparietal sulcus (**IPS**) including transverse parietal sulci
4. A cerebrospinal fluid (**CSF**) mask, obtained by masking the lateral ventricles manually, serving as control

Defining ROIs on an individual basis allowed us to work with high anatomical precision and avoided the need for spatial normalization.

2.5.3. Representational similarity analysis (RSA)

We employed an RSA to characterize the geometry of neural representations in frontal and parietal motor regions for imagined movements of varying perceived imagery vividness. These representational dissimilarity matrices (RDMs) represented the pairwise dissimilarity of activation patterns evoked by different imagined actions separately for rating-dependent groups of such patterns (see Fig. 1A).

Please note that due to the unpredictable behavior of each subject and the need for a random assignment of trials to specific groups, we had to perform the following steps ranging from *building rating groups* to *estimating brain RDMs* several times (from 25 to 58 repetitions between individuals) to compute an estimate of the true RDMs. We did this separately for each subject and each ROI.

2.5.3.1. Building rating groups. To compare imagined movements of varying perceived vividness, we grouped trials into eight bins based on the vividness ratings. We decided to create eight bins in order to maximize the variance of mean vividness ratings across these bins, while keeping enough trials per bin to enable a good estimate of fMRI data. Participants were instructed to confirm their rating with a key press. However, on some trials, they did not rate their perceived vividness resulting in a different number of rated trials between subjects (e.g., $rt = 52$ rated trials). To distribute the rated trials equally across rating groups, we divided the number of rated trials by 8 (*rem* $(52/8) = 4$). This gave us information about the number of trials that needed to be discarded in order to achieve an equal distribution. To avoid discarding trials from only one potential rating group, the respective number of rating groups was determined randomly (in this example, four rating groups: RG2, RG3, RG6, and RG8). This procedure avoided confounding effects on the rating groups due to an unbalanced discarding of trials across rating groups (e.g., the worst case in which 7 trials, which were all rated with 1 or 7, could be discarded). In the next step, we sorted all rated trials according to the rating (Fig. 1B.i) and put them into the eight bins while bearing in mind that a randomly picked rating group was allowed to have one more trial than the others (RG2, RG3, RG6, and RG8 contain seven trials, whereas RG1, RG4, RG5, and RG7 contain 6 trials, see Fig. 1B.ii). In the next step, we randomly picked one trial in each of the rating groups with one trial more than the others and deleted it from further analysis (Fig. 1B.iii). Because it was not unusual for the number of trials with a specific rating to exceed the amount of slots in a specific bin (e.g., 14 trials with a rating of six had to be distributed over Rating groups 6,7, and 8; see blue frame in Fig. 1B.iv), we again distributed the respective trials randomly. During all steps, we controlled for a balanced distribution of different movement types across rating groups. Because this whole procedure of generating the rating groups contained multiple randomization steps, it had to be repeated and averaged several times until the estimates converged (for more information, see *estimating brain RDMs* below). The resulting eight rating groups served as input conditions for the subsequent first-level analysis.

2.5.3.2. General linear models. In the next step, we computed a first-level analysis with SPM 12 using separate general linear models (GLMs) for each subject and each of the two sessions. We created nine boxcar regressors corresponding to the eight rating groups and the rest condition. The boxcar functions of each regressor spanned the imagery or rest interval (i.e., 8 s). The number of rest trials was chosen to match the number of trials in each rating group and was selected randomly. Each regressor was convoluted with a canonical hemodynamic response function. We also entered six movement parameters from the rigid-body

transformation of the motion-correction procedure as covariates in the GLM. We filtered the voxel-based time series with a high-pass filter (time constant = 128 s).

2.5.3.3. Generating representational dissimilarity matrices. We computed the representational dissimilarity matrices using the toolbox from Nili et al. (2014). Hence, we first estimated the true activity patterns by applying multivariate noise normalization to the beta coefficients obtained for the rating groups (Walther et al., 2016). Then, we calculated a cross-validated Mahalanobis distance reflecting the respective degree of dissimilarity for each pairwise rating group comparison, leading to an 8×8 RDM (Kriegeskorte et al., 2008). Cross validation was achieved by using the two sessions as inputs for a twofold cross-validation procedure. This yielded one brain RDM for each of the 13 ROIs per subject.

2.5.3.4. Estimating brain RDMs. By repeating the procedure of allocating trials to the appropriate bin by randomizing them followed by a first-level and representational similarity analysis, we created a further brain RDM for each ROI. After the second iteration, we again averaged the respective brain RDMs across all repetitions, leading to a mean brain RMD_n with n representing the number of iterations. Next, we calculated the correlation between the RDM_n and the $RDM_{(n-1)}$ in order to show how much the average $RDM_{(n-1)}$ changed when performing one more iteration. This helped us to estimate the minimal amount of iterations. The cutoff criterion was a correlation $\geq$0.99 three times in a row. We did this for each ROI, leading to an individual number of iterations (ranging from 25 to 58) and finally to one brain RDM for each subject and each ROI. After gaining the individual brain RDMs, we computed average RDMs across all subjects.

2.5.4. Association between rating behavior and its neural representation

We used two different analyses to investigate whether there was an association between the range of perceived vividness and the neuronal activity pattern. In a first step, we tested an association between the subjective perceived vividness and the geometry of neuronal representations that might cause them. For this purpose, we first created rating dissimilarity matrices (rating DMs) representing the structure of the rating groups in terms of their average vividness ratings. For each subject, we compared the mean group ratings to each other by calculating the absolute difference between them. This difference served as the dissimilarity, again leading to an 8×8 rating DM. We produced these rating DMs for each subject and each session separately (for more detailed illustrations see suppl. Fig. 1C). Furthermore, we created an average rating DM across both sessions for each subject.

We then tested whether there was a relationship between the overall average brain RDM (averaged across subjects) and the overall average rating DM to determine whether and how the variations between perceived vividness corresponded to the dissimilarities in neural activity patterns. We calculated Shepherd's *pi* correlation (Schwarzkopf et al., 2012) that first identifies outliers by bootstrapping the Mahalanobis distance and removing any outliers with a distance equal or larger than six. Then, we calculated Spearman's *rho* and adjusted the p value to account for the removal of outliers. We determined significance by using rating group label randomization and testing the null hypothesis that rating differences between rating groups would be independent of neural dissimilarity. This null hypothesis was simulated by a random permutation of the rating group labels and a computation of the randomized Shepherd correlations. The procedure was repeated 10,000 times, leading to a random distribution of correlations. The null hypothesis would be rejected if the correlation were to fall within the top 5% of the simulated null distributions of correlations. This was performed for each ROI separately, and p values were Holm–Bonferroni-corrected (1979).

2.5.5. Vividness dependency of neural pattern of imagined hand movements

Our next step was to perform a decoding analysis in order to test whether the specificity of the neural pattern of different imagined hand movements depended on vividness. Again, we separated imagery trials into different rating groups. Within these rating groups, we conducted a linear discriminant analysis (LDA) using a leave-one-run-out cross-validation for each subject together with the ROI based on functions taken from the MATLAB statistics toolbox. We tested whether the ability to differentiate between response patterns (i.e., decoding accuracy) of different imagined hand movements (aiming, extension–flexion, squeezing) depended on the rating group.

In contrast to the RSA, which estimated the neural activity by using several trials in a single regressor in the GLM, the decoding analysis was based on the neural activity pattern of single trials. Hence, the GLM was adjusted by creating one boxcar regressor for each single trial and then calculating this for each of the 20 runs. Again, we entered six movement parameters from the rigid-body transformation of the motion-correction procedure as covariates in the GLM per run, convoluted each regressor with a canonical hemodynamic response function, and filtered the voxel-based time series with a high-pass filter (time constant = 128 s). Then we applied multivariate noise normalization (Walther et al., 2016) resulting in the "true" activity patterns for each trial. Subsequently, we masked these activation patterns with each ROI and vectorized them. We z-scored the resulting feature vectors in order to avoid the influence of potential differences in mean amplitude and variance, and finally fed them into the decoding analysis.

2.5.5.1. Decoding imagined hand movements. Following a similar approach to that used in representational similarity analysis, we first created several rating groups containing an equal amount of trials of each type of hand movement. Again, these were created in order to maximize the variance of mean vividness ratings between the different rating groups and to keep a sufficient number of trials per rating group as training data for the classifier. We determined the number of rating groups by testing from four to eight rating groups. Again, the explicit assignment of trials to specific rating groups was not possible, so we applied an iterative approach. First, we sorted trials based on their ratings and assigned these to the rating groups—if needed, in a random manner. Next, within each rating group, we calculated the decoding accuracy using LDA and leave-one-run-out cross-validation. As previously described in Zabicki et al. (2016), LDA requires the dimensionality of the data to be lower than the number of training patterns provided. To reduce the number of features significantly below the number of training samples, we applied a principal components analysis (PCA) and used the first eight principal components (always capturing $\geq$ 60% of the variance in the data). In each iteration of the cross-validation, we split these vectors into a set of test (one feature vector of each action types) and training data (remaining feature vectors). The amount of cross-validation folds depended on the number of rating groups. In other words, fewer rating groups led to more trials within each group and therefore to more cross-validation folds. We gave the LDA algorithm labels indicating the action type for each of the training examples and derived a linear decision hyperplane on the basis of these data. We applied this decision criterion, in turn, to the test data and used it to assign action type labels to each of the three test vectors. We compared each of the assigned labels with the veridical labels and counted correct and incorrect assignments as 1 and 0 respectively. We then calculated the proportion of correct assignments across the folds of this cross-validation procedure. The proportion of correct assignments was derived separately for each subject, rating group, and ROI. After all these steps, the next iteration started by assigning the trials to the rating groups in a new randomized order.

2.5.5.2. Estimating decoding accuracies and testing for rating group effects. After each iteration, we averaged the calculated accuracy values (for each subject, rating group, and ROI) across all repetitions leading to a mean accuracy $mACC_n$, with n representing the number of iterations. To estimate the number of repetitions in order to obtain a good estimate of

the decoding accuracy independent of the explicit assignment of trials, we established a cutoffbreakup criterion: $mACC_n$ values of 1000 consecutive repetitions varied only within a range of 0.1% (cf. suppl. Fig. 2). This procedure led to an individual number of iterations (ranging from 2759 to 8813) and finally to an estimated decoding accuracy value for each subject, rating group, and ROI. Using these values, we conducted a repeated measures ANOVA for each ROI to test whether accuracy depended on rating group. Given a significant main effect for the rating group, post hoc pairwise comparisons (Tukey–Kramer-corrected) revealed which rating groups differed. This procedure was repeated for different numbers (from 3 to 8) of rating groups.

3. Results

3.1. Behavioral data: subjective ratings

All subjects gave rather high ratings in all experimental conditions (average median rating > 5.6) on a 7-point scale ranging from very high (7) to very low (1). A non-parametric Friedman test showed that vividness ratings do not differ between imagery of different hand movements, $\chi^2(2) = 3.364$, $p = 0.186$.

Individual differences in rating behavior were highly stable across two scanning sessions. Correlation analyses showed significant results for mean rating values ($r = 0.901$, $p < 0.0001$), variance ($r = 0.773$, $p < 0.0001$), and range ($r = 0.603$, $p < 0.01$) of rating (Fig. 2A). The distributions of the created rating groups showed an average (across all subjects) *RMSD* of 0.53 (*SEM* = 0.05). For detailed information, see suppl. Fig. 1B.

The analysis of rating behavior (Fig. 2B) revealed a strong within-subject correlation of rating DMs ($r = 0.71$, $p < 0.0001$), implying that subjects behaved similarly in both scanning sessions in terms of rating their perceived vividness of imagined movements. Despite a significant between-subject correlation ($r = 0.22$, $p < 0.0001$), indicating that participants tended to give high ratings, clearly individual rating characteristics were shown by the significant individualization value [*i* index = 0.49, *p*(average within-subject *r* > average between-subject *r*) < 0.0001], which was remarkably higher than the values reported by Charest et al. (2014).

3.2. Neuroimaging data

3.2.1. Representational similarity analysis (RSA)

For each ROI, we estimated the neural activity pattern during MI associated with the different vividness rating categories. This formed the input for the representational similarity analysis (RSA) (Kriegeskorte et al., 2008; Kriegeskorte and Kievit, 2013). We computed the representational dissimilarity for each rating pair as the multivariate noise-normalized and cross-validated Mahalanobis distance (Walther et al., 2016) between the respective neural patterns (Fig. 1). The resulting brain RDMs of the investigated ROIs and the control regions did not differ in the overall level of dissimilarities between the neural patterns elicited by different vividness rating groups (see Fig. 3 for the group average RDMs).

3.2.2. Is there an association between rating behavior and neural representation in frontal and parietal motor areas?

In a next step, we asked whether response-pattern geometries constitute the neural substrate of vividness impressions and the corresponding rating behavior. We found significant positive Shepherd's *pi* correlations (Holm–Bonferroni-corrected for 13 ROIs) between the average rating DM and the average brain RDM within left vPMC ($r = 0.80$, $p < 0.01$) and right IPL ($r = 0.65$, $p < 0.05$). This suggests that, within these regions, the neural dissimilarity corresponds to differences in the subjective vividness impression of specific rating groups (Fig. 4).

3.2.3. Is the decoding accuracy of imagined hand movements higher in more vivid trials?

We further asked whether the multivariate decoding of different imagined hand movements would differ in terms of the subjective vividness of the respective motor imagery trials. We took the given vividness ratings and created a specific number (from 4 to 8) of rating groups. The first *rating group* contained imagery trials with the lowest; the last *rating group*, with the highest vividness ratings. Within each group, we calculated accuracy values from the action decoding analysis and compared these between rating groups via repeated measures ANOVAs. We found similar main effects for each tested number of rating groups: The left vPMC as well as the right SPL showed the lowest *p* values and attained significance in almost every case (see Supplementary Fig. 3). Furthermore, we observed that the effect became lower for small as well as for large numbers of rating groups. Here, we report detailed results for six rating groups (all other results are reported in detail in suppl. Fig. 4). The analysis revealed a significant main effect of rating group on the decoding accuracy in left vPMC, $F(5, 95) = 3.59$, $p < 0.01$, $\eta^2 = 0.159$, and right SPL,($F(5, 95) = 3.78$, $p < 0.01$, $\eta^2 = 0.166$. Post hoc pairwise comparisons (Tukey–Kramer-corrected) revealed a significant difference between Rating group 2 and Rating group 4 for the left vPMC, as well as between Rating group 1 and Rating group 6 for the right SPL (Fig. 5).

4. Discussion

This study demonstrates that patterns of neural activity within the human motor cortices reflect the individual vividness of imagined actions as indicated by subjective ratings. Furthermore, our data reveal a connection between subjectively perceived vividness and the action specificity of the associated neural pattern. The correlation analysis compared the rating differences and the neural dissimilarity values of the rating groups separately for each region. It detected a significant positive correlation in the left vPMC and right IPL, indicating that these regions

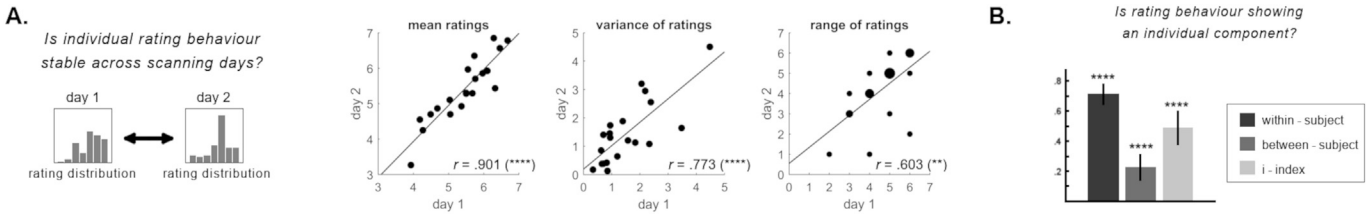

Fig. 2. Replicability of rating behavior. (A) Analyzing subjects' rating behavior by correlating mean ratings, variance of rating, and range of ratings between both scanning sessions. Significant correlations indicated by asterisks (*$p < 0.05$; **$p < 0.01$; ***$p < 0.001$; ****$p < 0.0001$; randomization analysis with 10,000 repetitions). (B) Comparing rating distributions of all subjects across scanning sessions. Rating behavior replicability (Pearson's *r*) is computed within subjects (dark gray bar) and between-subjects (light gray bar). Both are significant. The *i* index (orange bar) describes an individual unique component as the average within-subject replicability minus the average between-subject replicability. The *i* index is significant, indicating that different subjects have shown distinct rating behavior. Significance (****$p < 0.0001$, ***$p < 0.001$, **$p < 0.01$, *$p < 0.05$) of the within- and between-subject correlations was assessed by randomization of the rating value labels, whereas the significance of the *i* index was assessed by randomization of the subject labels. The error bar of the *i* index represents the SEM, estimated by bootstrap resampling of the set of subject pairs.

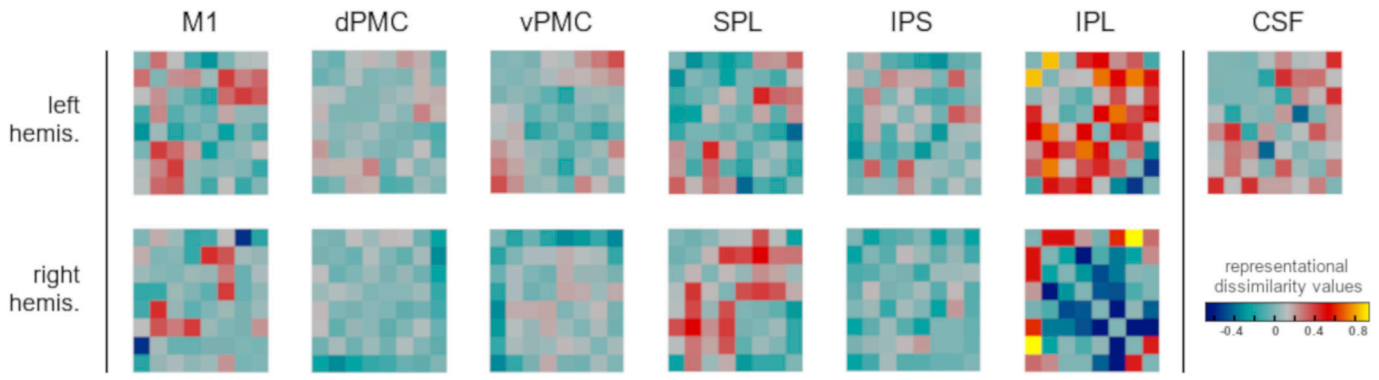

Fig. 3. Representational dissimilarity matrices of the brain data for every ROI. Shown RDMs are averaged across all subjects and contain in each cell the cross-validated Mahalanobis distance between each pair of the eight rating groups. M1: primary motor cortex, dPMC: dorsal premotor cortex, vPMC: ventral premotor cortex, SPL: superior parietal lobule, IPS: intraparietal sulcus, IPL: inferior parietal lobule, CSF: cerebrospinal fluid.

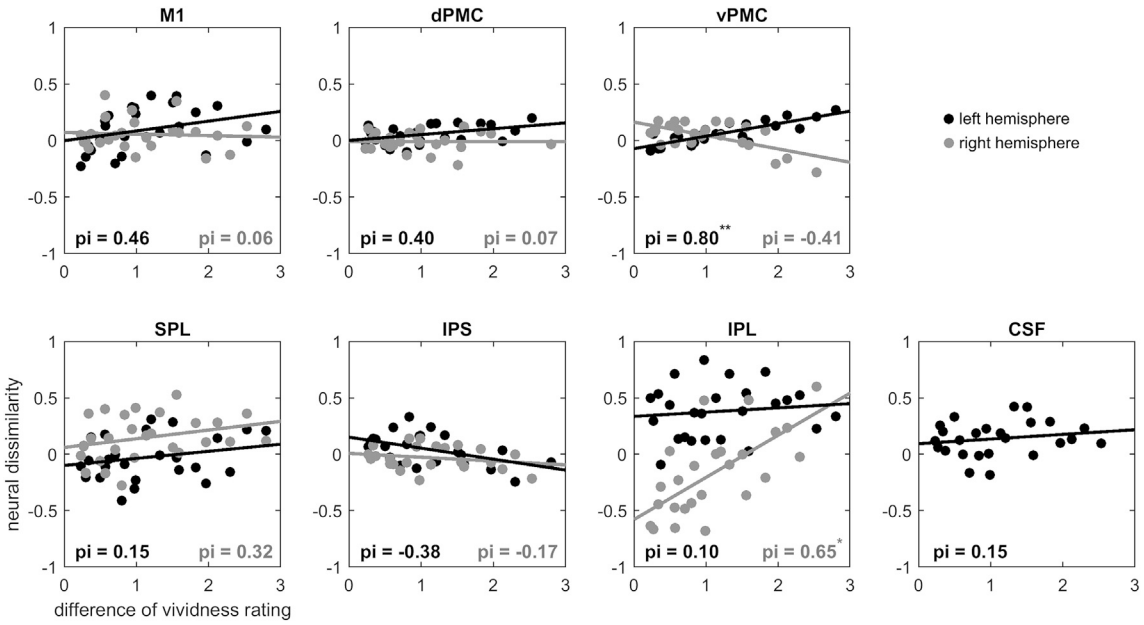

Fig. 4. Correlation between rating DMs and brain RDMs. Shepherd's *pi* correlation coefficients between each cell of the average rating DM and each cell of the average brain RDMs. Coefficients were calculated for each ROI. Significant correlations indicated by asterisks (*$p < 0.05$; **$p < 0.01$; randomization analysis with 10,000 repetitions). M1: primary motor cortex, dPMC: dorsal premotor cortex, vPMC: ventral premotor cortex, SPL: superior parietal lobule, IPS: intraparietal sulcus, IPL: inferior parietal lobule, CSF: cerebrospinal fluid.

particularly reflect perceived imagery vividness in the same way that similar rated trials evoke more similar neural patterns. Furthermore, the decoding analysis suggested that the vividness of the motor image relates systematically to the action specificity of neural activation patterns in left vPMC and right SPL. Imagined actions accompanied by higher vividness ratings are significantly more distinguishable from each other within these areas, suggesting that a vivid motor image correlates with a more distinct (cf. Zabicki et al., 2016) neural representation, which may reflect reduced levels of noise. This suggests that the quality of neural motor representations during imagery is linked directly to the perceived quality of the imagery process. Although our present results cannot reveal the source of this mechanism, we speculate that the reduced reliability of neural patterns associated with low-vividness imagery reflects neural noise associated with, for example, a lack of attention or the use of different imagery strategies (kinesthetic vs. visual imagery) (e.g., Guillot et al., 2009).

Following the suggestion of an anonymous reviewer, we performed further analysis within four additional ROIs by applying the same procedures as described in the manuscript. As suggested, we analyzed two prefrontal as well as two occipital ROIs, namely dorsolateral (DLPFC) and ventrolateral (VLPFC) prefrontal cortex as well as primary (V1) and secondary (V2) visual areas. All ROIs were created via the FreeSurfer parcellation algorithm. Visual regions were defined as the Brodman areas BA 17 (V1) and BA 18 (V2) whereas prefrontal ROIs were based on the Destrieux atlas (Destrieux et al., 2010), defining DLPFC as the middle frontal gyrus (mFG), and VLPFC as the triangular and opercular parts of the inferior frontal gyrus (c.f. Strangman et al., 2010). We found no effects with regard to the subjective vividness rating in these regions (see suppl. Fig 5): The similarity of neural patterns between different rating groups does not correlate with the difference of vividness ratings. Furthermore, decoding of different imagined hand movements in these regions does not depend on the given vividness rating. Thus, one might argue that the reported phenomenon seems to be a rather motor-related phenomenon.

Previous studies have proposed a dichotomy of good and bad imagery depending on the magnitude of neural activity in motor regions (Guillot et al., 2008; Lebon et al., 2012; Lorey et al., 2011; Mizuguchi et al., 2016). Our data significantly extend this view by showing that the geometry of neural population activity within motor regions reflects a dimension of low-to-high vividness, even for the limited range of overall

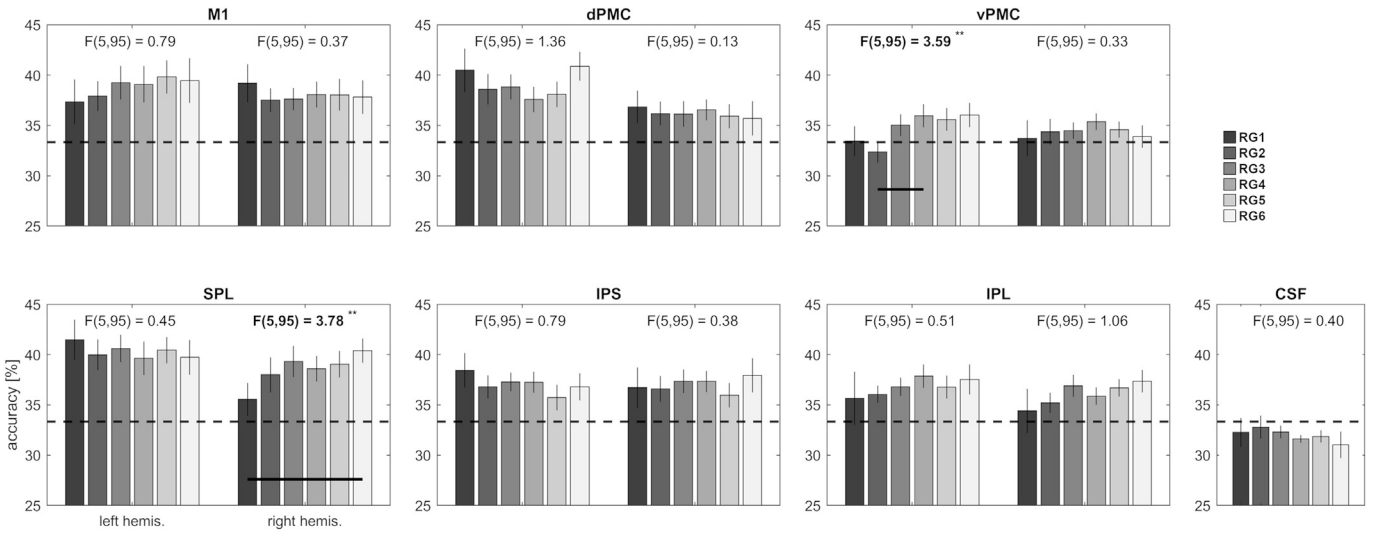

Fig. 5. Effect of degree of vividness on action decoding accuracy. Exemplary figure for six rating groups. Bars indicate average accuracy (error bar = SEM) when decoding different imagined hand movements within each rating group. Rating groups are characterized by perceived vividness level ranging from low (RG1) to high (RG6). For each ROI, a repeated measures ANOVA was conducted, investigating the main effect of vividness on decoding accuracy (as indicated by *F* values). Significant main effects displayed by asterisks (*$p < 0.05$; **$p < 0.01$). Significant post hoc pairwise comparisons (Tukey–Kramer-corrected) are indicated by a black horizontal line between the respective rating groups. Dashed line shows chance level. M1: primary motor cortex, dPMC: dorsal premotor cortex, vPMC: ventral premotor cortex, SPL: superior parietal lobule, IPS: intraparietal sulcus, IPL: inferior parietal lobule, CSF: cerebrospinal fluid.

relatively high ratings in our sample. This leads us to the following main conclusions: (a) Evoked patterns of neural activity within motor areas are shaped by imagery vividness. The present data provide evidence that motor representations are related to subjective impressions of this mental motor process. This relationship is statistically significant within the ventral section of the left PMC as well as the IPL of the right hemisphere. (b) The action specificity of neuronal patterns underlying motor imagery depends on vividness—a relationship that proves to be statistically significant within both the left vPMC and the right SPL. This suggests that the subjectively perceived vividness of a motor image is linked to a successful retrieval of specific features of its multimodal motor representation (i. e. including different qualities, for example visual and kinesthetic aspects).

Do vividness judgments arise from different patterns of neural activity in motor areas?

Previous studies have shown that MI is a simulation on the basis of motor representations (for a review, Jeannerod, 2001; Lotze and Halsband, 2006; Munzert et al., 2009). The ability to create vivid motor images can be considered to be an individual characteristic that varies within and between subjects on both a behavioral and a neural level (Guillot et al., 2008; Lorey et al., 2013; Olsson and Nyberg, 2010; Roberts et al., 2008). The present and former findings suggest that neural activation in terms of the magnitude of the bold response within the motor network, especially within parieto-premotor areas, varies inter- and intra-individually with perceived motor imagery vividness (Guillot et al., 2008; Lorey et al., 2011). In the present experiment, we found a close link between the representational geometry of activity patterns in motor areas and introspective ratings of vividness. This leads us to conclude that psychological assessments testing vividness of motor imagery and the underlying introspection actually do reflect properties of the underlying neural activity within premotor and posterior parietal areas. Thus, a very subjective aspect of an individual's experience is associated with observable patterns of neural activity in motor areas. Similar observations stem from the domain of vision and affective neuroscience (Chikazoe et al., 2014; Haxby et al., 2001). For example, Chikazoe et al. (2014) have demonstrated that the neural code of the orbito-frontal cortex (OFC) could classify experienced affect across participants and, therefore, showed that subjective impressions were retrievable from a pattern of regional neural activity.

We found a particularly pronounced relation between evoked patterns of neural activity and vividness within the ventral section of the left PMC as well as in right posterior parietal cortices such as the IPL and the SPL. These regions are thought to play a crucial role during MI (Decety et al., 1994; Gerardin et al., 2000; Nair et al., 2003; Stephan et al., 1995; Suchan et al., 2002). They are further known to contain internal body and action representations (built up by individual motor learning processes; see (Aziz-Zadeh and Damasio, 2008; Daprati et al., 2010) and are considered to induce motor awareness (Desmurget and Sirigu, 2009). The premotor cortex is involved in motor preparation, motor execution, and action planning. Furthermore, it is considered to subserve many higher-level aspects of movement planning such as the preparation and organization of movements and actions (Rizzolatti and Luppino, 2001; Wise, 1985) as well as action observation (Rizzolatti and Craighero, 2004). Especially the ventral section of the PMC is thought to be the core frontal region of the action mirror system (Rizzolatti and Craighero, 2004). Hence, it plays an important role in not only understanding the goal and the intention behind an observed action (Iacoboni et al., 2005) but also encoding more basic processes such as kinematics and motor features of observed actions (Fadiga et al., 2005; Rizzolatti and Craighero, 2004). The PPC is thought to be important for movement intention, decision making, and sensorimotor transformation (R. Andersen, 1989; Richard Andersen and Buneo, 2002; Buneo et al., 2002; Culham and Valyear, 2006; Desmurget et al., 2009; Graziano and Gross, 1998; Kalaska et al., 1997; Rizzolatti et al., 1997). However, the PPC is divided by the intraparietal sulcus (IPS) into a superior and an inferior section, the SPL and the IPL (Behrmann et al., 2004). Considering more specific functions of this subdivisions, it has been argued that one function of the SPL is to store internal models and action representations that are mandatory for action prediction as well as action simulation (Rizzolatti and Matelli, 2003; Winstein et al., 1997; Wolpert et al., 1998). For example, it has been demonstrated that the SPL carries information regarding the specific type of an imagined action (Pilgramm et al., 2016; Zabicki et al., 2016). In the present experiment, the decoding analysis revealed that imagined actions accompanied by higher vividness ratings are significantly more distinguishable from each other within the SPL. Thus, the retrieval of a distinct action-and goal-specific neuronal representation might be mandatory for the impression of a vivid motor image. Regarding the IPL, several fMRI studies have also emphasized the role of

this section in embodied simulation processes and prediction (Gallese, 2003, 2005; Keysers et al., 2004; Lorey et al., 2009; Rizzolatti and Craighero, 2004). A recent study by Lebon et al. (2018) examined associations between fMRI activation measured prior to MI training and kinesthetic or visual imagery strategies and their effect on motor performance in a finger sequence task. They observed that especially high kinesthetic imagery ability was associated with strong activation of the right IPL during MI before training. Therefore, the IPL was considered to be a key area while performing especially kinesthetic imagery. The present data showed that similar perceived imagery vividness evoked more similar neural patterns within this inferior section of the parietal cortex suggesting that the kinesthetic component also matters for the vividness impression.

Regarding the primary motor cortex, one might argue that the activation state of M1 is tuned by the activation state of the PMC, and, therefore, be also associated with subjective vividness. For example, several studies indicate that M1 neurons can hold premotor information for short periods, which suggests that M1 neurons might exhibit the functional equivalent of elementary memory functions (Alexander and Crutcher, 1990; Ashe et al., 1993; Georgopoulos et al., 1989; Kalaska and Crammond, 1992). It was further demonstrated that patterns of BOLD activation in M1 differentiate between types of imagined contralateral hand actions and thus underpin the importance of M1 for cognitive functions like MI (Pilgramm et al., 2016; Zabicki et al., 2016). However, the type of involvement of M1 during MI (especially with respect to the investigated task) is still controversial (Binkofski et al., 2000; Dechent et al., 2004; Hanakawa et al., 2003; Lotze et al., 1999; Porro et al., 1996; Porro et al., 2000). In this regard, for example, Kasess et al. (2008) applied DCM to data on MI and showed that the connection from SMA to M1 suppresses M1 activity during MI. The present analyses revealed no significant association between the subjectively attributed vividness and activity patterns within M1. The failure of this effect to reach statistical significance might be due to a weaker signal within M1 due to suppressed activation (Kasess et al., 2008). Further, the investigation of the relation between a subjective valuation of MI and neural activation and not the investigation of MI itself. One might speculate that such a higher-order process does not affect M1 activity by the same amount.

Is vivid motor imagery kinesthetic imagery?

The regions involved in MI may play separate roles for different aspects of imagery such as strategy or quality. For example, imagery strategies relate partly to the sensory modalities employed to imagine the action: kinesthetic (feeling of the movement) or visual (from a first- or third-person perspective). Accordingly, visual imagery is thought to require primarily the visual perception of the subject's movement in the mind's eye, whereas kinesthetic imagery is believed to be associated with motor functions, hence requiring subjects to imagine or to feel the movement while considering the body as a generator of forces. Guillot et al. (2009) compared these different imagery strategies directly. Alongside overlapping activation patterns, these authors described partially distinct networks for the different imagery strategies. When compared directly, they showed that the occipital regions (including the primary visual area and the extrastriate cortex) as well as superior parietal regions were recruited during visual imagery, whereas increased activity in the inferior parietal lobe as well as the ventral premotor cortex were observed during kinesthetic imagery. The present data revealed that neural pattern similarities within the ventral section of the premotor area as well as the inferior parietal lobe reflect rating scores on vividness of motor imagery. This suggests that vividness ratings may reflect the participant's ability to perform kinesthetic motor imagery and retrieve the respective motor representations including kinesthetic features (Guillot et al., 2009; Lebon et al., 2018). However, the present results also revealed that more vividly imagined hand movements are associated with more action-specific neuronal patterns within the left vPMC as well as the right SPL. Guillot et al. (2009) reported that the superior part of parietal cortex is more strongly linked to visual imagery. This suggests that vividness ratings may reflect both the kinesthetic and visual distinctiveness of an imagined action. Another possibility is that PPC activations may reflect a more abstract representation of the *goals* of the imagined actions (Pilgramm et al., 2016).

5. Conclusion

Our findings imply that measurements of neural activity in motor and motor-related areas represent differences in subjective experience of mental motor processes. Neural patterns within premotor and parietal areas exhibit a relationship with the vividness of self-generated motor images, especially within vPMC, IPL, and SPL. Moreover, increased vividness is accompanied by more distinct neural motor representation for imagined actions. This most probably reflects the degree of success regarding the kinesthetic (and possibly visual) retrieval of motor representations. Taken together, our findings link the subjective report of vividness of motor imagery to objective neurophysiological markers.

Declarations of interest

None.

Acknowledgements

The authors thank Carlo Blecker for his helpful support. We also thank Jonathan Harrow for native-speaker advice. AZ is a member of the International Training Group “The Brain in Action” (IRTG 1901) supported by the German Research Foundation (DFG). BdH was supported by a DFG research fellowship (HA 7574/1-1) and a JUST’US fellowship by JLU.

Appendix A. Supplementary data

Supplementary data to this article can be found online at https://doi.org/10.1016/j.neuroimage.2019.04.073.

References

Alexander, G.E., Crutcher, M.D., 1990. Preparation for movement: neural representations of intended direction in three motor areas of the monkey. J. Neurophysiol. 64 (1), 133–150.

Andersen, R., 1989. Visual and eye movement functions of the posterior parietal cortex. Annu. Rev. Neurosci. 12 (1), 377–403. https://doi.org/10.1146/annurev.neuro.12.1.377.

Andersen, Richard, Buneo, C.A., 2002. Intentional maps in posterior parietal cortex. Annu. Rev. Neurosci. 25, 189–220. https://doi.org/10.1146/annurev.neuro.25.112701.142922.

Ashe, J., Taira, M., Smyrnis, N., Pellizzer, G., Georgakopoulos, T., Lurito, J.T., Georgopoulos, A.P., 1993. Motor cortical activity preceding a memorized movement trajectory with an orthogonal bend. Exp. Brain Res. 95, 118–130. https://doi.org/10.1007/BF00229661.

Aziz-Zadeh, L., Damasio, A., 2008. Embodied semantics for actions: findings from functional brain imaging. J. Physiol. Paris 102 (1–3), 35–39. https://doi.org/10.1016/j.jphysparis.2008.03.012.

Baddeley, A.D., Andrade, J., 2000. Working memory and the vividness of imagery. J. Exp. Psychol. Gen. 129 (1), 126–145. https://doi.org/10.1037//0096-3445.129.1.126.

Behrmann, M., Geng, J.J., Shomstein, S., 2004. Parietal cortex and attention. Curr. Opin. Neurobiol. 14 (2), 212–217. https://doi.org/10.1016/j.conb.2004.03.012.

Binkofski, F., Amunts, K., Stephan, K.M., Posse, S., Schormann, T., Freund, H.-J., Seitz, R.J., 2000. Broca's region subserves imagery of motion: a combined cytoarchitectonic and fMRI study. Hum. Brain Mapp. 11, 273–285.

Braun, S.M., Kleynen, M., van Heel, T., Kruithof, N., Wade, D.T., Beurskens, A.J., 2013. The effects of mental practice in neurological rehabilitation; a systematic review and meta-analysis. Front. Hum. Neurosci. 7, 390. https://doi.org/10.3389/fnhum.2013.00390.

Buneo, C.A., Jarvis, M.R., Batista, A.P., Andersen, Richard, 2002. Direct visuomotor transformations for reaching. Nature 416, 632–636. https://doi.org/10.1038/416632a.

Charest, I., Kievit, R.A., Schmitz, T.W., Deca, D., Kriegeskorte, N., 2014. Unique semantic space in the brain of each beholder predicts perceived similarity. Proc. Natl. Acad. Sci. Unit. States Am. 111 (40), 14565–14570. https://doi.org/10.1073/pnas.1402594111.

Chikazoe, J., Lee, D., Kriegeskorte, N., Anderson, A.K., 2014. Population coding of affect across stimuli, modalities and individuals. Nat. Neurosci. 17 (8), 1114–1122. https://doi.org/10.1038/nn.3749.

Culham, J.C., Valyear, K.F., 2006. Human parietal cortex in action. Curr. Opin. Neurobiol. 16 (2), 205–212. https://doi.org/10.1016/j.conb.2006.03.005.
Daprati, E., Sirigu, A., Nico, D., 2010. Body and movement: consciousness in the parietal lobes. Neuropsychologia 48 (3), 756–762. https://doi.org/10.1016/j.neuropsychologia.2009.10.008.
Decety, J., Perani, D., Jeannerod, M., Bettinardi, V., Tadary, B., Woods, R.P., Fazio, F., 1994. Mapping motor representations with positron emission tomography. Nature 371, 600–602.
Dechent, P., Merboldt, K.-D., Frahm, J., 2004. Is the human primary motor cortex involved in motor imagery? Cogn. Brain Res. 19, 138–144. https://doi.org/10.1016/j.cogbrainres.2003.11.012.
Desmurget, M., Reilly, K.T., Richard, N., Szathmari, A., Mottolese, C., Sirigu, A., 2009. Movement intention after parietal cortex stimulation in humans. Science 324, 811–813. https://doi.org/10.1126/science.1169896.
Desmurget, M., Sirigu, A., 2009. A parietal-premotor network for movement intention and motor awareness. Trends Cognit. Sci. 13 (10), 411–419. https://doi.org/10.1016/j.tics.2009.08.001.
Destrieux, C., Fischl, B., Dale, A., Halgren, E., 2010. Automatic parcellation of human cortical gyri and sulci using standard anatomical nomenclature. Neuroimage 53 (1), 1–15. https://doi.org/10.1016/j.neuroimage.2010.06.010.
Ehrsson, H.H., Geyer, S., Naito, E., 2003. Imagery of voluntary movement of fingers, toes, and tongue activates corresponding body-part-specific motor representations. J. Neurophysiol. 90, 3304–3316. https://doi.org/10.1152/jn.01113.2002.
Fadiga, L., Craighero, L., Olivier, E., 2005. Human motor cortex excitability during the perception of others' action. Curr. Opin. Neurobiol. 15 (2), 213–218. https://doi.org/10.1016/j.conb.2005.03.013.
Feltz, D.L., Landers, D.M., 1983. The effects of mental practice on motor skill learning and performance: a meta-analysis. J. Sport Psychol. 5, 25–57.
Filimon, F., Rieth, C.A., Sereno, M.I., Cottrell, G.W., 2015. Observed, executed, and imagined action representations can be decoded from ventral and dorsal areas. Cerebr. Cortex 25, 3144–3158. https://doi.org/10.1093/cercor/bhu110.
Fogassi, L., Luppino, G., 2005. Motor functions of the parietal lobe. Curr. Opin. Neurobiol. 15, 626–631. https://doi.org/10.1016/j.conb.2005.10.015.
Gallese, V., 2003. The roots of empathy: the shared manifold hypothesis and the neural basis of intersubjectivity. Psychopathology 36 (4), 171–180. https://doi.org/10.1159/000072786.
Gallese, V., 2005. Embodied simulation: from neurons to phenomenal experience. Phenomenol. Cognitive Sci. 4, 23–48.
Georgopoulos, A.P., Crutcher, M.D., Schwartz, A.B., 1989. Cognitive spatial-motor processes: 3. Motor cortical prediction of movement direction during an instructed delay period. Exp. Brain Res. 75, 183–194. https://doi.org/10.1007/BF00248541.
Gerardin, E., Sirigu, A., Lehericy, S., Poline, J.-B., Gaymard, B., Marsault, C., Le Bihan, D., 2000. Partially overlapping neural networks for real and imagined hand movements. Cerebr. Cortex 10, 1093–1104. https://doi.org/10.1093/cercor/10.11.1093.
Graziano, M.S.A., Gross, C.G., 1998. Spatial maps for the control of movement. Curr. Opin. Neurobiol. 8, 195–201. https://doi.org/10.1016/S0959-4388(98)80140-2.
Grezes, J., Decety, J., 2001. Functional anatomy of execution, mental simulation, observation, and verb generation of actions: a meta-analysis. Hum. Brain Mapp. 12, 1–19.
Guillot, A., Collet, C., Nguyen, V.A., Malouin, F., Richards, C.L., Doyon, J., 2008. Functional neuroanatomical networks associated with expertise in motor imagery. Neuroimage 41, 1471–1483.
Guillot, A., Collet, C., Nguyen, V.A., Malouin, F., Richards, C.L., Doyon, J., 2009. Brain activity during visual versus kinesthetic imagery: an fMRI study. Hum. Brain Mapp. 30, 2157–2172. https://doi.org/10.1002/hbm.20658.
Hanakawa, T., Immisch, I., Toma, K., Dimyan, M.A., van Gelderen, P., Hallett, M., 2003. Functional properties of brain areas associated with motor execution and imagery. J. Neurophysiol. 89 (2), 989–1002. https://doi.org/10.1152/jn.00132.2002.
Haxby, J.V., Ida Gobini, M., Furey, M., Ishai, A., Schouten, J., Pietrini, P., 2001. Distributed and overlapping representations of faces and objects in ventral temporal cortex. Science 293 (5539), 2425–2430.
Haynes, J.-D., 2011. Decoding and predicting intentions. Ann. N. Y. Acad. Sci. 1224, 9–21. https://doi.org/10.1111/j.1749-6632.2011.05994.x.
Heed, T., Beurze, S.M., Toni, I., Roder, B., Medendorp, W.P., 2011. Functional rather than effector-specific organization of human posterior parietal cortex. J. Neurosci. 31 (8), 3066–3076. https://doi.org/10.1523/JNEUROSCI.4370-10.2011.
Holm, S., 1979. A simple sequentially rejective multiple test procedure. Scand. J. Stat. 6, 65–70.
Hutton, C., Bork, A., Josephs, O., Deichmann, R., Ashburner, J., Turner, R., 2002. Image distortion correction in fMRI: a quantitative evaluation. Neuroimage 16, 217–240. https://doi.org/10.1006/nimg.2001.1054.
Iacoboni, M., Molnar-Szakacs, I., Gallese, V., Buccino, G., Mazziotta, John, Rizzolatti, G., 2005. Grasping the intentions of others with one's own mirror neuron system. PLoS Biol. 3 (3), e79. https://doi.org/10.1371/journal.pbio.0030079.
Isaac, A.R., 1992. Mental practice - does it work in the field? Sport Psychol. 6, 192–198.
Isaac, A.R., Marks, D., 1994. Individual differences in mental imagery experience: developmental changes and specialization. Br. J. Psychol. 85, 479–500.
Jeannerod, M., 2001. Neural simulation of action: a unifying mechanism for motor cognition. Neuroimage 14, S103–S109. https://doi.org/10.1006/nimg.2001.0832.
Kalaska, J.F., Crammond, D.J., 1992. Cerebral cortical mechanisms of reaching movements. Science 255 (5051), 1517–1523.
Kalaska, J.F., Scott, S.H., Cisek, P., Sergio, L.E., 1997. Cortical control of reaching movements. Curr. Opin. Neurobiol. 7, 849–859. https://doi.org/10.1016/S0959-4388(97)80146-8.
Kamitani, Y., Tong, F., 2005. Decoding the visual and subjective contents of the human brain. Nat. Neurosci. 8 (5), 679–685. https://doi.org/10.1038/nn1444.
Kasess, C.H., Windischberger, C., Cunnington, R., Lanzenberger, R., Pezawas, L., Moser, E., 2008. The suppressive influence of SMA on M1 in motor imagery revealed by fMRI and dynamic causal modeling. Neuroimage 40, 828–837. https://doi.org/10.1016/j.neuroimage.2007.11.040.
Keysers, C., Wicker, B., Gazzola, V., Anton, J.-L., Fogassi, L., Gallese, V., 2004. A touching sight: SII/PV activation during the observation and experience of touch. Neuron 42, 335–346. https://doi.org/10.1016/S0896-6273(04)00156-4.
Kriegeskorte, N., Kievit, R.A., 2013. Representational geometry: integrating cognition, computation, and the brain. Trends Cognit. Sci. 17 (8), 401–412. https://doi.org/10.1016/j.tics.2013.06.007.
Kriegeskorte, N., Mur, M., Bandettini, P.A., 2008. Representational similarity analysis - connecting the branches of systems neuroscience. Front. Syst. Neurosci. 2, 4. https://doi.org/10.3389/neuro.06.004.2008.
Lebon, F., Byblow, W.D., Collet, C., Guillot, A., Stinear, C.M., 2012. The modulation of motor cortex excitability during motor imagery depends on imagery quality. Eur. J. Neurosci. 35 (2), 323–331. https://doi.org/10.1111/j.1460-9568.2011.07938.x.
Lebon, F., Horn, U., Domin, M., Lotze, M., 2018. Motor imagery training: kinesthetic imagery strategy and inferior parietal fMRI activation. Hum. Brain Mapp. 39 (4), 1805–1813. https://doi.org/10.1002/hbm.23956.
Lorey, B., Bischoff, M., Pilgramm, S., Stark, R., Munzert, J., Zentgraf, K., 2009. The embodied nature of motor imagery: the influence of posture and perspective. Exp. Brain Res. 194, 233–243. https://doi.org/10.1007/s00221-008-1693-1.
Lorey, B., Naumann, T., Pilgramm, S., Petermann, C., Bischoff, M., Zentgraf, K., Munzert, J., 2013. How equivalent are the action execution, imagery, and observation of intransitive movements? Revisiting the concept of somatotopy during action simulation. Brain Cogn. 81, 139–150. https://doi.org/10.1016/j.bandc.2012.09.011.
Lorey, B., Naumann, T., Pilgramm, S., Petermann, C., Bischoff, M., Zentgraf, K., Munzert, J., 2014. Neural simulation of actions: effector- versus action-specific motor maps within the human premotor and posterior parietal area? Hum. Brain Mapp. 35, 1212–1225. https://doi.org/10.1002/hbm.22246.
Lorey, B., Pilgramm, S., Bischoff, M., Stark, R., Vaitl, D., Kindermann, S., Zentgraf, K., 2011. Activation of the parieto-premotor network is associated with vivid motor imagery - a parametric fMRI study. PLoS One 6 (5), e20368. https://doi.org/10.1371/journal.pone.0020368.
Lotze, M., Halsband, U., 2006. Motor imagery. J. Physiol. 99, 386–395. https://doi.org/10.1016/j.jphysparis.2006.03.012.
Lotze, M., Montoya, P., Erb, M., Hülsmann, E., 1999. Activation of cortical and cerebellar motor areas during executed and imagined hand movements: an fMRI study. J. Cogn. Neurosci. 11 (5), 491–501.
Mantani, T., Okamoto, Y., Shirao, N., Okada, G., Yamawaki, S., 2005. Reduced activation of posterior cingulate cortex during imagery in subjects with high degrees of alexithymia: a functional magnetic resonance imaging study. Biol. Psychiatry 57, 982–990. https://doi.org/10.1016/j.biopsych.2005.01.047.
Mizuguchi, N., Nakata, H., Kanosue, K., 2016. Motor imagery beyond the motor repertoire: activity in the primary visual cortex during kinesthetic motor imagery of difficult whole body movements. Neuroscience 315, 104–113. https://doi.org/10.1016/j.neuroscience.2015.12.013.
Munzert, J., Lorey, B., Zentgraf, K., 2009. Cognitive motor processes: the role of motor imagery in the study of motor representations. Brain Res. Rev. 60, 306–326. https://doi.org/10.1016/j.brainresrev.2008.12.024.
Munzert, J., Zentgraf, K., 2009. Motor imagery and its implications for understanding the motor system. In: Progress in Brain Research. Mind and Motion: the Bidirectional Link between Thought and Action, vol. 174. Elsevier, pp. 219–229. https://doi.org/10.1016/S0079-6123(09)01318-1.
Murphy, S.M., 1994. Imagery interventions in sport. Med. Sci. Sports Exerc. 26 (4), 486–494.
Nair, D.G., Purcott, K.L., Fuchs, A., Steinberg, F., Kelso, J.A.S., 2003. Cortical and cerebellar activity of the human brain during imagined and executed unimanual and bimanual action sequences: a functional MRI study. Cogn. Brain Res. 15, 250–260.
Nili, H., Wingfield, C., Walther, A., Su, L., Marslen-Wilson, W., Kriegeskorte, N., 2014. A toolbox for representational similarity analysis. PLoS Comput. Biol. 10 (4), e1003553. https://doi.org/10.1371/journal.pcbi.1003553.
Oldfield, R.C., 1971. The assessment and analysis of handedness: the Edinburgh inventory. Neuropsychologia 9, 97–113.
Olsson, C.-J., Nyberg, L., 2010. Motor imagery: if you can't do it, you won't think it. Scand. J. Med. Sci. Sports 20, 711–715. https://doi.org/10.1111/j.1600-0838.2010.01101.x.
Park, C.-H., Chang, W.H., Lee, M., Kwon, G.H., Kim, L., Kim, S., Kim, Y.-H., 2015. Which motor cortical region best predicts imagined movement? Neuroimage 113, 101–110. https://doi.org/10.1016/j.neuroimage.2015.03.033.
Pilgramm, S., de Haas, B., Helm, F., Zentgraf, K., Stark, R., Munzert, J., Krüger, B., 2016. Motor imagery of hand actions: decoding the content of motor imagery from brain activity in frontal and parietal motor areas. Hum. Brain Mapp. 37, 81–93. https://doi.org/10.1002/hbm.23015.
Porro, C.A., Cettolo, V., Francescato, M.P., Baraldi, P., 2000. Ipsilateral involvement of primary motor cortex during motor imagery. Eur. J. Neurosci. 12, 3059–3063. https://doi.org/10.1046/j.1460-9568.2000.00182.x.
Porro, C.A., Francescato, M.P., Cettolo, V., Diamond, M.E., Baraldi, P., Zuiani, C., Di Prampero, P.E., 1996. Primary motor and sensory cortex activation during motor performance and motor imagery: a functional magnetic resonance imaging study. J. Neurosci. 16 (23), 7688–7698.
Rizzolatti, G., Craighero, L., 2004. The mirror-neuron system. Annu. Rev. Neurosci. 27, 169–192. https://doi.org/10.1146/annurev.neuro.27.070203.144230.
Rizzolatti, G., Fogassi, L., Gallese, V., 1997. Parietal cortex: from sight to action. Curr. Opin. Neurobiol. 7, 562–567.

Rizzolatti, G., Luppino, G., 2001. The cortical motor system. Neuron 31, 889–901. https://doi.org/10.1016/S0896-6273(01)00423-8.

Rizzolatti, G., Matelli, M., 2003. Two different streams form the dorsal visual system: anatomy and functions. Exp. Brain Res. 153, 146–157. https://doi.org/10.1007/s00221-003-1588-0.

Roberts, R., Callow, N., Hardy, L., Markland, D., Bringer, J., 2008. Movement imagery ability: development and assessment of a revised version of the vividness of movement imagery questionnaire. J. Sport Exerc. Psychol. 30, 200–221.

Schwarzkopf, D.S., de Haas, B., Rees, G., 2012. Better ways to improve standards in brain-behavior correlation analysis. Front. Hum. Neurosci. 6, 200. https://doi.org/10.3389/fnhum.2012.00200.

Stephan, K.M., Fink, G.R., Passingham, R.E., Silbersweig, D., Ceballos-Baumann, A.O., Frith, C.D., Frackowiak, R.S.J., 1995. Functional anatomy of the mental representation of upper extremity movements in healthy subjects. J. Neurophysiol. 73 (1), 373–386.

Strangman, G.E., O'Neil-Pirozzi, T.M., Supelana, C., Goldstein, R., Katz, D.I., Glenn, M.B., 2010. Regional brain morphometry predicts memory rehabilitation outcome after traumatic brain injury. Front. Hum. Neurosci. 4 (182). https://doi.org/10.3389/fnhum.2010.00182.

Suchan, B., Yágüez, L., Wunderlich, G., Canavan, A.G.M., Herzog, H., Tellmann, L., Seitz, R.J., 2002. Neural correlates of visuospatial imagery. Behav. Brain Res. 131, 163–168. https://doi.org/10.1016/S0166-4328(01)00373-4.

Walther, A., Nili, H., Ejaz, N., Alink, A., Kriegeskorte, N., Diedrichsen, J., 2016. Reliability of dissimilarity measures for multi-voxel pattern analysis. Neuroimage 137, 188–200. https://doi.org/10.1016/j.neuroimage.2015.12.012.

Winstein, C., Grafton, S.T., Pohl, P.S., 1997. Motor task difficulty and brain activity: investigation of goal-directed reciprocal aiming using positron emission tomography. J. Neurophysiol. 77, 1581–1594.

Wise, S.P., 1985. The primate premotor cortex: past, present, and preparatory. Annu. Rev. Neurosci. 8, 1–19.

Wolpert, D.M., Goodbody, S.J., Husain, M., 1998. Maintaining internal representations: the role of the human superior parietal lobe. Nat. Neurosci. 1 (6), 529–533.

Zabicki, A., de Haas, B., Zentgraf, K., Stark, R., Munzert, J., Krüger, B., 2016. Imagined and Executed Actions in the Human Motor System: Testing Neural Similarity between Execution and Imagery of Actions with a Multivariate Approach. Cerebral Cortex. Advance online publication. https://doi.org/10.1093/cercor/bhw257.